Original Article

Enhancing chondrogenic potential via mesenchymal stem cell sheet multilayering

Hallie Thorp [a, b], Kyungsook Kim [a, *], Sophia Bou-Ghannam [a, b], Makoto Kondo [a], Travis Maak [c], David W. Grainger [a, b], Teruo Okano [a, d, **]

[a] Cell Sheet Tissue Engineering Center (CSTEC), Department of Pharmaceutics and Pharmaceutical Chemistry, University of Utah, Salt Lake City, UT, USA
[b] Department of Biomedical Engineering, University of Utah, Salt Lake City, UT, USA
[c] Department of Orthopaedic Surgery, University of Utah, Salt Lake City, UT, USA
[d] Institute of Advanced Biomedical Engineering and Science, Tokyo Women's Medical University, TWIns, Japan

ARTICLE INFO

ABSTRACT

Advanced tissue engineering approaches for direct articular cartilage replacement in vivo employ mesenchymal stem cell (MSC) sources, exploiting innate chondrogenic potential to fabricate hyaline-like constructs in vitro within three-dimensional (3D) culture conditions. Cell sheet technology represents one such advanced 3D scaffold-free cell culture platform, and previous work has shown that 3D MSC sheets are capable of in vitro hyaline-like chondrogenic differentiation. The present study aims to build upon this understanding and elucidate the effects of an established cell sheet manipulation technique, cell sheet multilayering, on fabrication of MSC-derived hyaline-like cartilage 3D layered constructs in vitro. To achieve this goal, multilayered MSC sheets are prepared and assessed for structural and biochemical transitions throughout chondrogenesis. Results support MSC multilayering as a means of increasing construct thickness and 3D cellular interactions related to in vitro chondrogenesis, including N-cadherin, connexin 43, and integrin β-1. Data indicate that increasing construct thickness from 14 μm (1-layer construct) to 25 μm (2-layer construct) increases these cellular interactions and subsequent in vitro MSC chondrogenesis. However, a clear initial thickness threshold (33 μm - 3-layer construct) is evident that decreases the rate and extent of in vitro chondrogenesis, specifically chondrogenic gene expressions (Sox9, aggrecan, type II collagen) and sulfated proteoglycan accumulation in deposited extracellular matrix (ECM). Together, these data support the utility of cell sheet multilayering as a platform for tailoring construct thickness and subsequent MSC chondrogenesis for future articular cartilage regeneration applications.

© 2021, The Japanese Society for Regenerative Medicine. Production and hosting by Elsevier B.V. This is an open access article under the CC BY-NC-ND license (http://creativecommons.org/licenses/by-nc-nd/4.0/).

1. Introduction

Articular cartilage is an avascular and aneural tissue exhibiting minimal intrinsic ability to regenerate without intervention [1,2].

Due to this limited healing ability, articular cartilage defects are common precursors for developing or accelerating onset of osteo-arthritis (OA), which is challenging to treat successfully once degeneration has begun [3,4]. As healthy articular cartilage exhibits hyaline structure and characteristics, therapies that immediately replace this hyaline cartilage at the site of chondral defects are increasingly being developed [1,5–7].

Tissue engineering attempts to recreate or regenerate tissues mimicking native host tissue and is a common platform for developing this type of hyaline cartilage replacement therapy [8–10]. Growing efforts within tissue engineering aim to employ mesenchymal stem cells (MSC) as an allogeneic cell source offering well-documented regenerative properties, standards for preparing cells with specific phenotypes, and multipotency, including

* Corresponding author. Cell Sheet Tissue Engineering Center (CSTEC), Department of Pharmaceutics and Pharmaceutical Chemistry, Health Sciences, University of Utah, 30 South 2000 East, Salt Lake City, UT 84112, USA. Fax: +1 801 581 3674.
** Corresponding author. Cell Sheet Tissue Engineering Center (CSTEC), Department of Pharmaceutics and Pharmaceutical Chemistry, Health Sciences, University of Utah, 30 South 2000 East, Salt Lake City, UT 84112, USA. Fax: +1 801 581 3674.
E-mail addresses: kyungsook.kim@utah.edu (K. Kim), teruo.okano@utah.edu (T. Okano).

chondrogenic lineages [11—14]. To achieve MSC chondrogenic differentiation, three-dimensional (3D) culture conditions and 3D cellular interactions are known to be essential [15—19]. Compared to traditional two-dimensional (2D) adherent cell culture, 3D culture platforms allow cells to assume rounded morphologies and promote increased pro-chondrogenic cellular interactions [16,17,20]. Extensive work has been reported for tailoring 3D scaffold-based and scaffold-free platforms for in vitro MSC chondrogenesis to fabricate transplantable hyaline-like cartilage. However, to date, none have achieved reliable clinical translation, due in part to difficulties in reliably differentiating to phenotypically and functionally desirable hyaline cartilage in vitro or in vivo [1,6,21].

As a unique scaffold-free platform, cell sheet tissue engineering, pioneered by Okano et al. uses temperature-responsive cultureware to produce 3D cell sheet constructs that retain endogenous cellular environments, cell matrix, receptors, and adhesive proteins, permitting spontaneous sheet adhesion to biologic surfaces without supporting materials [22—27]. Previous work from our group has shown that 3D MSC sheets are capable of producing hyaline-like cartilage in vitro that directly adheres to cartilage surfaces [28]. These 3D MSC sheets were able to strongly adhere directly to cartilage surfaces after achieving chondrogenic differentiation, determined via immunohistochemical staining and qualitative assessments [26]. Relative to 2D culture conditions, 3D MSC sheets exhibited increased expression of pro-chondrogenic extracellular matrix (ECM) markers and cellular interactions prior to induction, in turn promoting enhanced hyaline-like chondrogenesis in vitro [28]. Current cell sheet applications seek to build upon these previous chondrogenic differentiation successes by further enhancing 3D cellular interactions via cell sheet manipulation.

Cell sheet manipulation techniques, such as multilayering, have been shown to increase construct thickness and cellular interactions for a variety of cell types and therapeutic applications [29—33]. Specifically, for cartilage regeneration applications, multilayered chondrocyte sheets expressed enhanced cellular interactions and type II collagen accumulation in the ECM relative to single-layer sheets [34—36]. In vitro multilayering of endometrial cell sheets likewise showed increased glycosaminoglycan (GAG) and collagen expressions relative to non-layered sheets [37]. Based on the chosen cell source and desired final construct characteristics, a range of multilayering techniques have been developed, including non-assisted, weighted, centrifugation, and gelatin stamp manipulations [29,32,38—40]. Cell sheet multilayering techniques applied to chondrogenic MSC sheets should therefore enhance requisite 3D cellular interactions to increase in vitro MSC chondrogenic capacity and hyaline-like phenotypes in multilayered constructs.

This study investigates the effects of cell sheet multilayering on fabrication of hyaline-like cartilage constructs from MSCs in vitro. Based on previous cell sheet studies, we hypothesize that multilayering will increase cellular interactions within resultant thick-tissue MSC constructs, in turn influencing in vitro chondrogenic differentiation. Therefore, we evaluated changes in structure and cellular interaction within MSC sheets following multilayering, as well as assessed the subsequent hyaline-like transitions throughout in vitro chondrogenic differentiation. The present study verifies the utility of this cell sheet manipulation technique to further develop MSC-derived hyaline-like scaffold-free cartilage transplants for future articular cartilage regeneration therapies.

2. Materials and methods

2.1. Cell culture and cell sheet fabrication

Human whole bone marrow-derived mesenchymal stem cells (hBMSCs) were isolated from human bone marrow aspirate purchased from Lonza (product number: PT2501) according to previously verified methods [41]. Briefly, bone marrow aspirates were suspended in growth media containing High-Glucose (4.5 g/L) Dulbecco's Modified Eagle's Medium (HG-DMEM) (Life Technologies, USA) supplemented with 10% fetal bovine serum (FBS) (Thermo Fisher Scientific, USA), 0.1 mM nonessential amino acids (NEAA) (Life Technologies, USA), 1% penicillin streptomycin (PS) (Gibco, USA), and 1 ng/mL basic fibroblast growth factor (bFGF) (PeproTech, USA). Suspended aspirates were plated at 5×10^3 cells/cm^2 on tissue culture plastic and incubated in a humidified environment (37 °C, 5% CO_2). hBMSCs were selected based on adherence to the tissue culture plastic and non-adherent cells were washed away during media changes. Tissue culture flasks were rocked gently every day to ensure only adherent cells were attaching to culture surfaces and media was changed twice per week. Once the hBMSCs were ~90% confluent, approximately 2 weeks, they were harvested using 0.05% Trypsin—EDTA (Gibco), counted using a hemocytometer, and frozen or plated for continued culture.

For culture, hBMSCs were plated at 3000 cells/cm^2 in growth media containing HG-DMEM supplemented with 10% FBS, 1% PS, and 1 ng/mL bFGF and incubated in a humidified environment (37 °C, 5% CO_2). Media was changed at day 1 and day 3, and cells were cultured until 90% confluent, approximately 5 days. Cells were passaged using 0.05% Trypsin—EDTA and the cell suspensions were counted using a hemocytometer. Cells were expanded and banked at Passage 2 and 4 and used for experimentation at Passage 6. For cell sheet fabrication, Passage 6 cells were plated onto 35 mm diameter UpCell temperature-responsive cell culture dishes (TRCD) (CellSeed, Tokyo, Japan) in 10% FBS growth media additionally supplemented with 50 μg/mL ascorbic acid at a seeding density of 6×10^5 cells/sheet. Cell sheets were cultured for 5 days, with no media changes, until cells reached confluence. At 5 days, cell sheets were moved to 20 °C (room temperature (RT)) for 20 min, then detached with forceps.

2.2. Cell sheet layering

Before re-plating and/or layering cell sheets, 1.0 μm-diameter pore, 6-well cell culture inserts (Falcon, USA) were conditioned with FBS overnight to aid in adhesion. Inserts were washed twice with 1 × phosphate buffered saline (PBS) (Gibco) to remove residual FBS before sheet transfer.

To layer sheets without centrifugation, detached cell sheets were transferred to the conditioned cell culture inserts using overhead projector polyester film (Apollo, NY, USA) to ensure basal contact with insert well culture surfaces. Growth media volume was adjusted to 5 μL and sheets were incubated in a humidified environment (37 °C, 5% CO_2) for 1 h. After 1 h, the second cell sheet was detached from the TRCD, manually transferred onto the bottom cell sheet using the overhead projector polyester film, and aligned with the bottom sheet by pipetting. Media volume was adjusted to 5 μL and 2-layer constructs were incubated in a humidified environment (37 °C, 5% CO_2) for 1 h before fresh media was added. Layered constructs in fresh media were incubated for 3 days to promote attachment.

To layer sheets with centrifugation, detached cell sheets were transferred to the conditioned cell culture inserts using overhead projector polyester film (Apollo). The insert well membranes were then trimmed around the attached cell sheet and transferred to 35-mm cell culture dishes (CELLTREAT, USA) with forceps. Media volume was adjusted to 5 μL and cell sheet dishes were centrifuged (Eppendorf 5810R fitted with a A-4-81 rotor) for 5 min at 38 °C, 800 rpm (114 rcf), with ramped acceleration/deceleration. For 2-layer constructs, a second cell sheet was transferred onto the

centrifuged sheet using overhead projector polyester film and aligned by pipetting. Layered constructs were incubated in a small volume of media (10–20 μL) for 30 min in a humidified environment (37 °C, 5% CO_2). After 30 min, 2-layer constructs were centrifuged for 5 min at 38 °C, 800 rpm (114 rcf), with ramped acceleration/deceleration. For 3-layer sheets, a third cell sheet was transferred onto the centrifuged 2-layer sheets using overhead projector polyester film and aligned by pipetting. Layered constructs were incubated in a small volume of media for 30 min in a humidified environment (37 °C, 5% CO_2), then centrifuged for 5 min at 38 °C, 800 rpm (114 rcf), with ramped acceleration/deceleration. After centrifugation, layered cell sheet constructs on insert membranes were transferred to fresh 1.0 μm-diameter pore, 6-well cell culture inserts, fresh cell growth media was added, and constructs were incubated (37 °C, 5% CO_2) for an additional 3 days to ensure attachment. All cell sheet constructs were imaged macroscopically with a handheld camera (Canon sX280 HS) immediately after layering and after 3-day incubation to visually assess quality of layered sheets (i.e. no holes, non-attached sections, or shifting had occurred during processing).

2.3. Cell sheet chondrogenic differentiation

After the 3-day incubation, chondrogenic samples were induced with chondrogenic medium and transferred to a hypoxia incubator (37 °C, 5% CO_2, 5% O_2). Chondrogenic medium contained HG-DMEM supplemented with 10 ng/mL transforming growth factor beta-3 (TGFβ3) (Thermo Fisher Scientific), 200 ng/mL bone morphogenetic protein-6 (BMP6) (PeproTech), 1% Insulin-Transferrin-Selenium (ITS-G) (Thermo Fisher Scientific), 1% PS (Life Technologies), 1% NEAA (Thermo Fisher Scientific), 100 nM dexamethasone (MP Biomedicals, OH, USA), 1.25 mg/mL bovine serum albumin (BSA) (Sigma–Aldrich, MO, USA), 50 μg/mL L-ascorbic acid 2-phosphate (Sigma–Aldrich), 40 μg/mL L-proline (Sigma–Aldrich), and 5.35 μg/mL linoleic acid (Sigma–Aldrich). Media composition was based on previously reported components and concentrations [28], and media was changed twice a week for the duration of differentiation (day-0 − 3-weeks).

2.4. Histological analysis

For histological analysis, samples were fixed with 4% paraformaldehyde (PFA) (Thermo Scientific) for 15 min, paraffin embedded, and sectioned at 4 μm thicknesses. For all staining and cell counting, at least 2 slides were stained per replicate ($n \geq 3$ biological replicates via at least 2 experimental repetitions) to provide suitable sample sizes. To identify cell morphology, Hematoxylin and Eosin (H&E) staining was conducted according to standard methods [42]. Briefly, samples were stained for 4 min with Mayer's Hematoxylin (Sigma–Aldrich), then 4 min with Eosin (Thermo Scientific). To detect mature chondrogenesis via sulfated proteoglycan content in the ECM, Safranin-O staining was conducted according to standard methods [42]. Briefly, samples were stained for 4 min with Wiegert's Iron Hematoxylin, 5 min with 0.5 g/L Fast Green, and 5 min with 0.1% Safranin-O (all Sigma-–Aldrich). All samples were affixed with a coverslip and dried overnight before being imaged with a BX 41 widefield microscope (Olympus, Japan) using AmScope Software (v4.8.15934, USA). H&E-stained cross sections were used to calculate cell sheet thicknesses and nuclei densities. For each cell sheet slide, three pictures were taken along the length of the cell sheet. Using the measurement tools built into the AmScope software, five measurements from the apical to basal edge of the sheet were made per picture, and these measurements were evenly spaced out along the sheet. Nuclei counting was performed using the same 3 pictures/sheet. Using the

measurement tools built into the AmScope software, a 500 μm length of the cell sheet was marked and the number of nuclei were counted within the marked section using ImageJ software (v.1.51, U. S. National Institutes of Health, MD, USA). Nuclei density was calculated as average number of nuclei per average area (thicknesses × 500 μm length) for corresponding images.

2.5. Real-time quantitative PCR analysis

RNA from samples was extracted using 1 mL TRIzol/sample (Ambion, Life Technologies, CA, USA) with a pestle motor mixer. Total RNA was isolated with the PureLink RNA Mini Kit (Invitrogen, Thermo Fisher Scientific) according to manufacturer instructions. For cDNA synthesis, all comparative samples were synthesized at the same time. Before synthesizing cDNA, the RNA was quantified with a NanoDrop spectrophotometer (Thermo Scientific, USA), and all cDNA samples were prepared from 1 μg of RNA/sample. All samples with a purity (A_{260}/A_{280}) greater than 1.8 were deemed pure enough to use. cDNA synthesis was conducted using a High-Capacity cDNA Reverse Transcriptase Kit (Applied Biosystems, Thermo Fisher Scientific, MA, USA) as per manufacturer instructions. Real-time quantitative PCR analysis was conducted with TaqMan Universal PCR Master Mix (Applied Biosystems, Thermo Fisher Scientific) using an Applied Biosystems Step-OnePlus instrument. Gene expression levels were analyzed for the following genes: glyceraldehyde 3-phosphate dehydrogenase (GAPDH, Hs99999905_m1) as a housekeeping gene, β-catenin (Hs00355049_m1), N-cadherin (Hs00983056_m1), integrin β1 (Hs01127536_m1), connexin 43 (Hs04259536_g1), SRY-box 9 (SOX9, Hs01001343_g1), collagen type II alpha 1 chain (COL2, Hs00264051_m1), collagen type I alpha 1 chain (COL1, Hs00164004_m1). All primers were manufactured by Applied Biosystems. Relative gene expression was calculated by the quantitative comparative CT method [43]. Gene expressions were normalized to GAPDH expression levels and relative to the 0-day single-layer cell sheet group.

2.6. Statistical analysis

All statistical analysis was completed using GraphPad Prism software (v.9, https://www.graphpad.com/scientific-software/prism/) with data sets of $n \geq 3$ biological replicates via at least 2 experimental repetitions and incorporating technical replicates to ensure consistency of results [43]. All quantitative values are expressed as mean ± standard deviation (SD). All data sets were checked for normality using a Shapiro–Wilk test. Data sets comparing 3 or more groups were analyzed using a one-way analysis of variance (ANOVA) and either Bonferroni or Tukey's testing depending on normality results (Figs. 2 and 3). Statistical significance was determined for time comparison data using a series of one-way ANOVA (Figs. 4B and 5). To evaluate significance in single variable comparison data sets, two-tailed, unpaired student t-tests were used after confirming normality of data using the Shapiro–Wilk test (Fig. 4C). Statistical significance was defined as not significant (ns) $p \geq 0.05$, *$p < 0.05$, **$p < 0.01$, ***$p < 0.001$.

3. Results

3.1. Cell sheet layering methods create cohesive interfaces

Cultured human whole bone marrow-derived mesenchymal stem cell (hBMSC) sheets were successfully layered both with and without centrifugation, but were unable to create an immediate cohesive sheet–sheet interface without centrifugation (Fig. 1). Macroscopic top-down images of centrifuged and non-centrifuged 2-layer constructs showed no significant differences in size or

shape (Fig. 1A and B), with both layered constructs remaining physically intact for 3 days post-layering and during fixation and paraffin block preparation. Cross-sectional Hematoxylin & Eosin (H&E) histological analysis revealed that the non-centrifuged 2-layer constructs exhibited significant gaps between the apical and basal sheets, indicating weak interfacing (Fig. 1C). The centrifuged 2-layer constructs showed few to no gaps between the sheets, creating a complete and cohesive interface (Fig. 1D). Therefore, all further layering experimentation for chondrogenesis utilized the centrifugation layering technique.

3.2. Post-layering changes in cell sheet thickness and cellular density

Cultured hBMSC sheets were successfully layered with centrifugation to form 1-layer (1L), 2-layer (2L), and 3-layer (3L) constructs (Fig. 2A—C). Multilayered hBMSC constructs 3 days post-layering showed increases in construct thickness with increasing layer numbers: 1-layer (14.46 ± 3.69 µm), 2-layer (25.59 ± 5.22 µm), 3-layer (32.83 ± 5.71 µm) (Fig. 2D). Each additional cell sheet layer significantly increased construct thickness ($p = 0.0003$ (1L:2L); 0.0093 (2L:3L); <0.0001 (1L:3L)). 2-layer and 3-layer constructs showed 1.77-fold and 2.27-fold increases in thickness compared to 1-layer, respectively. Nuclei density increased with additional layers, but density differences were only significantly increased in 3-layer compared to 1-layer constructs (Fig. 2E) ($p = 0.3584$ (1L:2L); 0.5689 (2L:3L); 0.0419 (1L:3L)). Number of cells within a 500 µm cross-section also increased significantly, although not linearly, with each additional cell sheet layer (Fig. 2F) ($p = 0.0003$ (1L:2L); 0.0097 (2L:3L); <0.0001 (1L:3L)).

3.3. Post-layering changes in cell sheet cellular interactions

In addition to structural changes during cell sheet layering, changes in gene expression associated with cellular interactions were seen before chondrogenic induction (Fig. 3). Relative gene expressions of cell-ECM interaction marker integrin β-1 (Fig. 3C)

and gap junction marker connexin 43 (Fig. 3D) significantly increased in 2-layer and 3-layer constructs compared to 1-layer (Integrin β-1: $p = 0.0024$ (1L:2L); 0.0003 (2L:3L); <0.0001 (1L:3L); Connexin-43: $p = 0.0151$ (1L:2L); 0.0001 (2L:3L); <0.0001 (1L:3L)). Layered constructs (2-layer and 3-layer) showed significantly increased N-cadherin expression relative to 1-layer constructs ($p = 0.0003$ (1L:2L); 0.0012 (1L:3L)), but expression was not significantly different between the 2-layer and 3-layer constructs (Fig. 3B) ($p = 0.2444$ (2L:3L)). Additionally, no significant differences were seen among the relative gene expression for β-catenin in all groups (1-, 2-, and 3-layer) (Fig. 3C).

3.4. Histological changes in chondrogenic multilayered hBMSC sheets

hBMSCs were chosen as an MSC source with documented chondrogenic potential [13,28], and 3-week chondrogenic differentiation of hBMSCs prepared as 1-layer cell sheets resulted in positive hyaline-like chondrogenesis (Fig. 4A) similar to previously reported results [28]. Positive Safranin-O staining was not identified in 1-, 2-, or 3- layered constructs before chondrogenic induction (Figs. 4A—0 day). Safranin-O stains sulfated proteoglycans red (depth of red color relative to GAG content) with Fast Green counterstaining other ECM blue-green. Accumulation of sulfated proteoglycans in the ECM increased for all layered constructs over the course of 3-week differentiation. Expression of slightly positive Safranin-O staining was observed by 1-week post-induction for 1-layer and 2-layer constructs, but not until 2-weeks post-induction for 3-layer constructs. Similarly high levels of sulfated proteoglycan staining and lacunae structures were expressed in 3-week differentiated 1-layer and 2-layer constructs, whereas the 3-week differentiated 3-layer constructs remained weakly positive for hyaline-like phenotypes (Fig. 4A). The thickness of all layered constructs (1-, 2-, and 3-layers) increased during differentiation (3-week compared to 0-day) (Fig. 4B). Relative thickness increases between 0-day and 3-weeks for 1-layer, 2-layer, and 3-layer constructs showed 18.89-fold, 11.41-fold, and 7.87-fold increases,
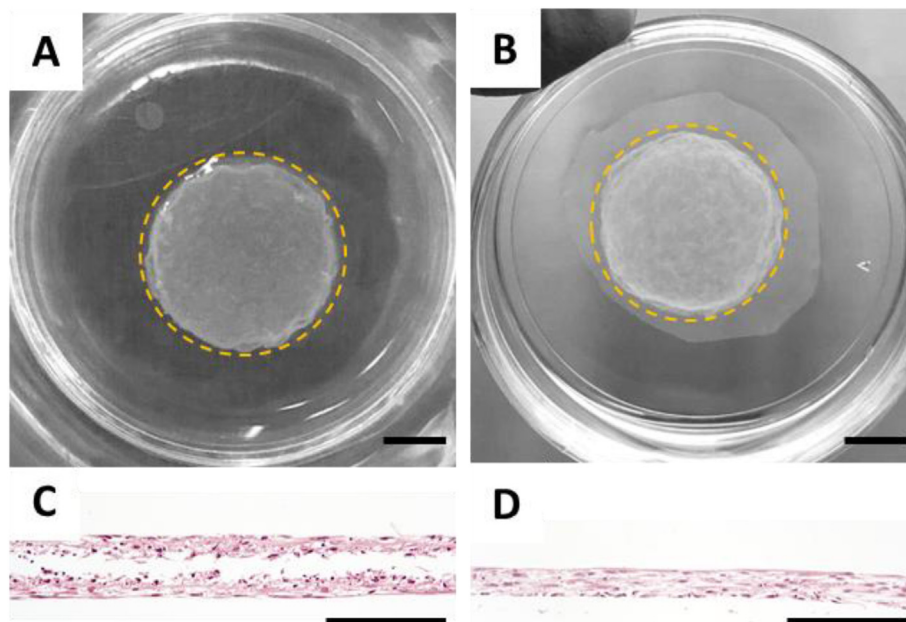

Fig. 1. Cell sheet multi-layering with and without centrifugation observed macroscopically and histologically. Representative macroscopic images of 2-layer hBMSC sheets (A) without centrifugation and (B) with centrifugation. Dotted orange line denotes the periphery of the cell sheets. Representative cross-sectional H&E histology for 2-layer cell sheets (C) without centrifugation and (D) with centrifugation, 3 days post-layering. Scale bars: (A,B) 5 mm, (C,D) 200 µm.
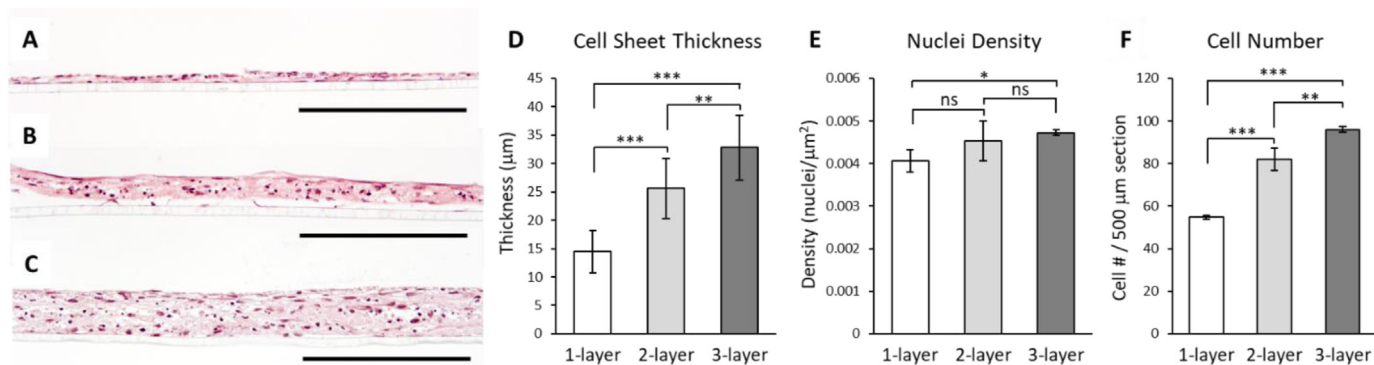
Fig. 2. Effects of cell sheet multi-layering on construct thickness and nuclear density. Representative cross-sectional H&E histology for (A) 1-layer, (B) 2-layer, and (C) 3-layer cell sheets 3 days post-layering. Scale bars: 250 μm. Cell construct (D) thickness, (E) cellular density, and (F) cell numbers (per 500 μm cross-section) for 1-, 2-, and 3-layer cell sheets 3 days post-layering, prior to chondrogenic induction. Error bars represent means ± SD (ns: $p > 0.05$; *$p < 0.05$; **$p < 0.01$; ***$p < 0.001$).
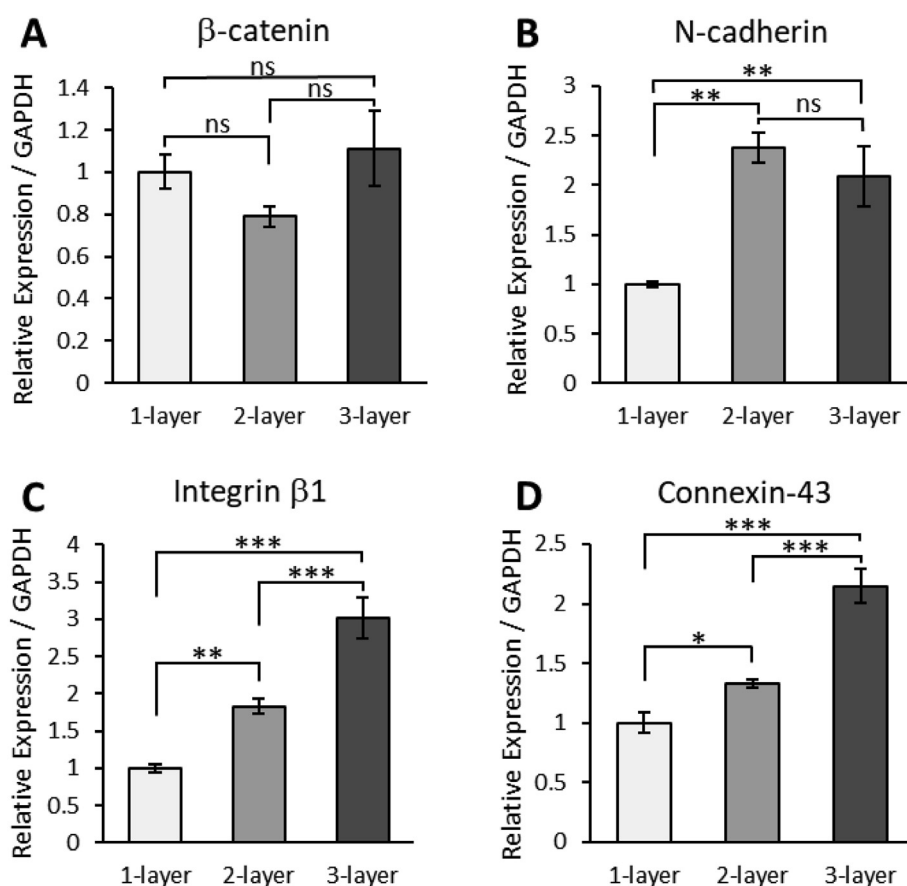

Fig. 3. Gene expression comparisons for cellular interactions in 1-, 2-, and 3-layer constructs. Quantitative real-time PCR gene expression in 1-, 2-, and 3-layer sheets 3 days post-layering for cell−cell markers (A) β-catenin and (B) N-cadherin, cell-ECM marker (C) Integrin b1, and gap junction marker (D) Connexin 43. All gene expression normalized to GAPDH and compared to the 1-layer control sample. Error bars represent means ± SD (ns: $p > 0.05$; *$p < 0.05$; **$p < 0.01$; ***$p < 0.001$).

respectively. Chondrogenic differentiation of 2-layer constructs result in significantly thicker constructs at 1-week and 2-week timepoints compared to 1-layer or 3-layer constructs (p = <0.0001 (1L:2L 1W); <0.0001 (2L:3L 1W); 0.0014 (1L:2L 2W); 0.0001 (2L:3L 2W)) (Fig. 4B). However, fold changes in thicknesses throughout chondrogenesis indicated similar early ECM deposition abilities in 1-layer and 2-layer constructs (7.69-fold increase (0-day:1W 1L); 7.04-fold increase (0-day:1W 2L)). Changes in cell numbers (number of cells per 500 μm cross-sections) between 0-day and 3-weeks differentiation were not significant for any

layered constructs (Fig. 4C) (p = 0.070 (0-day:3W 1L); 0.109 (0-day:3W 2L); 0.222 (0-day:3W 3L)), indicating that increases in thickness result from ECM deposition rather than cellular proliferation.

3.5. Hyaline-like gene expression in chondrogenic multilayered hBMSC sheets

Gene expression data supported variable hyaline-like characteristics among the layered constructs (Fig. 5). For early
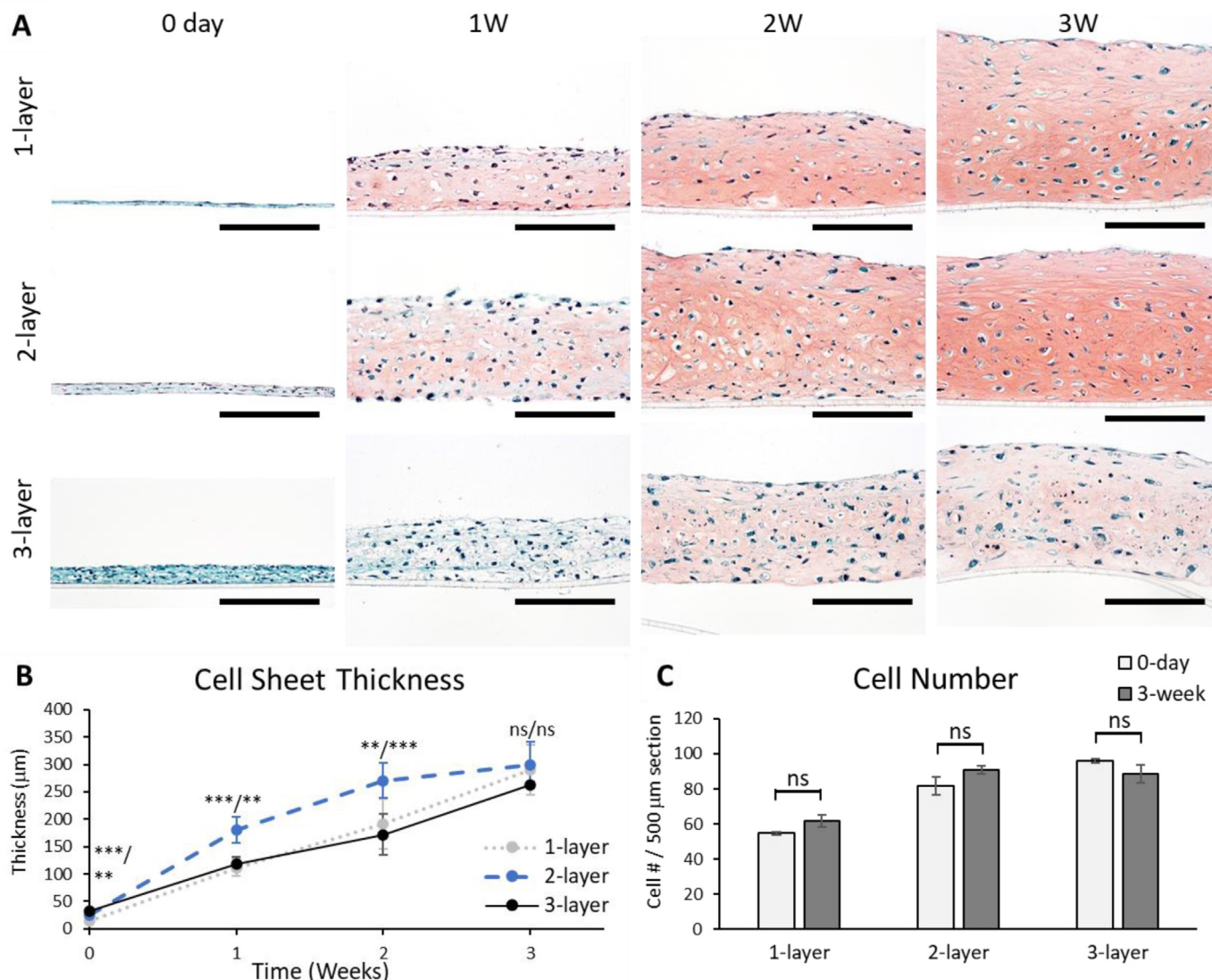
Fig. 4. Structural and phenotypic changes in multi-layered hBMSC constructs throughout chondrogenesis. (A) Representative cross-sectional Safranin-O histology to identify sulphated proteoglycans for 1-layer, 2-layer, and 3-layer cell sheets in chondrogenic medium for 0 days to 3 weeks (3W). Scale bars: 250 μm. Cell construct (B) thickness for 1-layer (dotted grey), 2-layer (dashed blue), and 3-layer sheets (solid black) in chondrogenic medium for 0 days to 3 weeks. (C) Comparative cell numbers (per 500 μm cross-section) for 1-layer, 2-layer, and 3-layer sheets at 0-day (light grey) and 3-weeks (dark grey) differentiation. Error bars represent means ± SD (ns: $p > 0.05$; **$p < 0.01$; ***$p < 0.001$). (B) Statistical analysis p values are represented as 1-layer vs. 2-layer/2-layer vs. 3-layer.

chondrogenic marker SRY-Box Transcription Factor 9 (Sox9), relative gene expression was similarly positive in 1-layer and 2-layer constructs ($p = 0.8855$ (1L:2L 1W); 0.091 (1L:2L 2W)); significantly higher than in 3-layer constructs at 1-week and 2-week timepoints ($p = 0.0035$ (1L:3L 1W); 0.0023 (2L:3L 1W); 0.0016 (1L:3L 2W); 0.0195 (2L:3L 2W)) (Fig. 5A). For mature chondrogenic marker aggrecan (ACAN), relative gene expression was significantly higher in 1-layer constructs at 1-week and 2-weeks relative to 2- and 3-layer constructs (Fig. 5B) ($p = 0.0073$ (1L:2L 1W); <0.0001 (1L:3L 1W); 0.0013 (1L:2L 2W); <0.0001 (1L:3L 2W)). At 1- and 2-weeks differentiation, aggrecan expression was significantly higher in 2-layer relative to 3-layer constructs (Fig. 5B) ($p = 0.0019$ (2L:3L 1W); 0.0049 (2L:3L 2W)). Aggrecan expression at 3 weeks was not significantly different among all groups ($p = 0.9812$ (1L:2L); 0.3073 (2L:3L); 0.2449 (1L:3L)). Type II collagen expression was likewise significantly higher in 1-layer constructs compared to 2-layer or 3-layer constructs at 1-week and 2-week timepoints ($p = <0.0001$ (1L:2L 1W); <0.0001 (1L:3L 1W); 0.0475 (1L:2L 2W); 0.0061 (1L:3L

2W)). Type II collagen expression was also significantly higher in 2-layer constructs compared to 3-layer constructs at 1-week timepoints (Fig. 5C) ($p = 0.0001$). Type II collagen expression at 3 weeks was not significantly different among all groups ($p = 0.8844$ (1L:2L); 0.2510 (2L:3L); 0.4394 (1L:3L)). While type II collagen gene expression was not significantly different between 1-layer and 2-layer constructs at 3-weeks, the type II to type I collagen gene expression ratio was significantly higher in the 2-layer constructs, indicating possibly more hyaline-like phenotypes (Fig. 5D). The type II-to-type I collagen ratio was significantly higher in the 1-layer and 2-layer constructs relative to the 3-layer constructs at 1-week. At 2-week differentiation, the collagen ratio for the 2-layer constructs was significantly higher than the 1-layer constructs, which was significantly higher than the 3-layer constructs ($p = 0.0287$ (1L:2L 2W); 0.0112 (1L:3L 2W)). By 3-weeks differentiation, the collagen ratio for the 2-layer constructs was significantly greater than the 1-layer and 3-layer constructs ($p = 0.0052$ (1L:2L 3W); 0.001 (2L:3L 3W)).
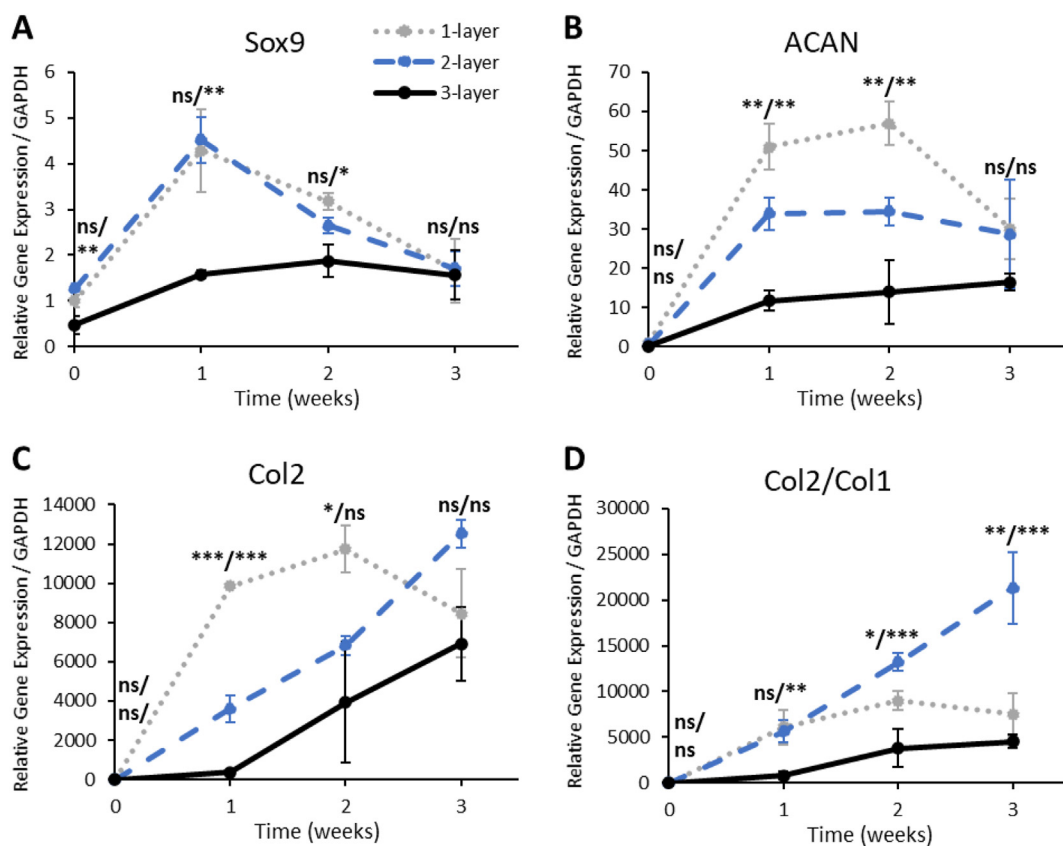
Fig. 5. Gene expression comparisons for chondrogenic potential in 1-, 2-, and 3-layer constructs. Quantitative real-time PCR of 1-layer (dotted grey), 2-layer (dashed blue), and 3-layer sheets (solid black) for chondrogenic gene expression: (A) Sox9, (B) aggrecan (ACAN), and (C) type II collagen (Col2) from 0-day to 3-weeks chondrogenesis. (D) Ratios of type II to type I collagen (Col2/Col1) for 1-, 2-, and 3-layer sheets shown as ratios of relative gene expression from 0-day to 3-weeks chondrogenesis. All gene expression normalized to GAPDH and compared to the 1-layer 0-day control samples. Error bars represent means ± SD (ns: $p > 0.05$; *$p < 0.05$; **$p < 0.01$; ***$p < 0.001$). Statistical analysis p values are represented as 1-layer vs. 2-layer/2-layer vs. 3-layer.

4. Discussion

3D culture conditions are known to influence induction and maintenance of MSC hyaline-like chondrogenic differentiation in vitro [15,16,44,45]. Within 3D culture conditions, cells are able to take on more rounded morphologies compared to 2D conditions, establishing more direct cellular interactions with surrounding and immediately adjacent cells required for chondrogenesis [16,20,46,47]. Specifically within cell sheet tissue engineering, cellular interactions have been shown to increase following cell sheet transitions from 2D to 3D conditions, suggesting that enhanced cellular interactions may be associated with increases in thicknesses or cellular densities of the resultant 3D tissue [28,48]. In the present study, multilayered MSC sheets show similar significant increases in expression of cellular interaction molecules (Fig. 3B–D). This significant upregulation of cellular interactions in layered constructs is most likely attributed to cellular distribution within the thicker 3D layered constructs. Within these detached, contracted, 3D constructs, the flattened cells at the construct periphery interact with ECM and adjacent cells only in some directions (towards the middle of the cell sheet), compared to the more rounded internal cells fully surrounded and in direct contact in all directions. The construct's thickness increases with additional cell sheet layers (Fig. 2D), without detectably altering the diameters of the cell sheets. As such, the peripheral cell populations are expected to remain similar, with increasing proportions of internal relative to peripheral cells as the contrast thickness increases, resulting in an increased overall population of cells establishing

enhanced cell-ECM and cell–cell interactions. From these results, we can reaffirm that cell sheet multilayering is a valuable tool for controlling construct thickness and increasing 3D cellular interactions prior to chondrogenic induction, without necessitating increased cellular densities.

Proposed relationships between cellular interactions and in vitro MSC chondrogenesis have been extensively published previously [16,17,49–52]. Notably, certain cellular interactions are modulated via β-catenin, N-cadherin, integrin β1, and connexin 43, playing essential roles during early chondrogenesis, primarily in regulating cellular condensation and early chondrogenic commitment [49–52]. Cell sheet technology has similarly shown that increased cellular interactions prior to chondrogenic induction, most likely stimulated by spontaneous post-detachment cell sheet contraction, facilitate in vitro hyaline-like chondrogenesis in 3D MSC sheets [28]. In those 3D cell sheets, compared to 2D cell cultures, transitions to three-dimensionality and increases in 3D cellular interactions prior to chondrogenic induction were linked to increases in ECM deposition and accumulation of type II collagen and sulfated proteoglycans in the deposited ECM; common hallmarks of hyaline-like chondrogenesis [5,9,28]. In the present study, MSC sheet multilayering further increases pro-chondrogenic 3D cellular interactions with additional cell sheet layers (Fig. 3). Compared to the previously reported single-layer 3D cell sheets, multilayered constructs presented here allow more tailored increases in construct thickness, subsequently affording more control over requisite pro-chondrogenic cellular interactions. Specifically, increased gene expressions of connexin 43, a gap–junction

precursor, and integrin β1, a cell-ECM interaction marker, suggest more direct pathways for cellular communication and transduction of chondrogenic cues among adjacent cells in multilayered constructs [49,50,53]. Gene expression of β-catenin, a cell–cell and cell migration marker, was not significantly increased in layered structures, most likely because of limited changes in cellular migration potential in the cell-dense, ECM-rich cell sheets following multilayering [54,55]. Additionally, β-catenin localizes to the nucleus when activated via canonical Wingless/Int (Wnt)/β-catenin signaling cascades, or the cell membrane when inactivated [56,57]. Gene expression analysis does not selectively differentiate between nuclear- and membrane-localized β-catenin; therefore, the similar gene expressions in layered constructs may still result in variable activation of Wnt/β-catenin signaling cascades during chondrogenic induction based on β-catenin localization. Taken together, these data suggest that MSC constructs comprising more cell sheet layers, with increased 3D cellular interactions, should induce more rapid or more hyaline-like subsequent chondrogenesis.

Data shown in Figs. 4 and 5 support this hypothesis and identify an optimal thickness for the hyaline-like chondrogenic differentiation of hBMSC sheets. The extent of hyaline-like differentiation increased from 1-layer (~14 μm thickness) to 2-layer constructs (~25 μm thickness), evidenced by chondrogenic ECM deposition (Fig. 4) and resultant type II/type I collagen gene expressions (Fig. 5D) seen in 3-week differentiated 2-layer constructs. A clear MSC layered construct thickness threshold also emerged, where thicker structures (3-layered constructs (~33 μm thickness)) dramatically decreased the rate and extent of hyaline-like differentiation compare to 1- and 2-layer constructs (Figs. 4 and 5). This notable decrease in chondrogenic potential suggests that relative chondrogenic capacity of 3D MSC sheets is directly related to the initial construct thickness.

A primary limitation hindering the hyaline-like differentiation of the 3-layer constructs, relative to the 1- and 2-layer constructs, may be oxygen and nutrient diffusion through the thicker tissue. Other studies have found that in thicker tissues, increased oxygen and nutrient diffusion gradients significantly diminish chondrogenic differentiation, cellular viability, and cellular functionality [58–61]. For chondrogenic cell sheet applications, future work may therefore choose to adjust cell sheet diameters to decrease diffusion distance, or employ bioreactors to increase convective transport via forced diffusion, to confirm the influence of construct thickness on diffusion-related chondrogenesis, and increase the thickness thresholds to produce thicker-tissue hyaline-like cartilage constructs [59,60,62]. Additionally, the number of cells within the layered constructs increases with additional cell sheet layers (Fig. 2F), which may also impact the nutrient diffusion through the thicker constructs as there are more cells consuming the same amount of available media. Furthermore, although cell numbers did not significantly change during differentiation, the number of cells in 3-layer sheets did slightly decrease (Fig. 4C); therefore, it is possible that diminished chondrogenic potential of the 3-layer constructs could also be related to cell loss during fabrication and/or differentiation. Although there is a clear initial thickness threshold for producing hyaline-like cartilage constructs from the presented hBMSC sheets, increased hyaline-like characteristics, specifically type II/type I collagen gene expressions and sulfated proteoglycan-rich ECM in the 2-layer constructs, ultimately indicate that cell sheet multilayering within certain initial thickness constraints can be used to enhance hyaline-like differentiation of MSCs in vitro.

Cell sheet layering techniques allow variable control over construct thickness and cellular densities [29,31–33,38], which were hypothesized to influence in vitro MSC chondrogenesis.

Confirming this hypothesis, this study demonstrates that 1) MSC sheet layering increases 3D cellular interactions within the resultant thick-tissue constructs, and 2) initial construct thickness thresholds affect rate and extent of MSC chondrogenic potential. Based on these findings, we assert that cell sheet technology and multilayering techniques present a valuable platform for tailoring construct thickness and subsequent MSC chondrogenesis to further develop optimized in vitro hyaline-like scaffold-free cartilage transplants for future focal chondral defect regeneration.

5. Conclusion

Cell sheet multilayering presented in this study represents an important strategy for specifically increasing construct thickness and enhancing 3D cellular interactions related to in vitro MSC chondrogenesis. We have shown that 2-layer cell sheet constructs develop the most hyaline-like structures in the presence of differentiation media in vitro, due in part to suitable initial construct thicknesses and enhanced cellular interactions. These data highlight the importance of closely regulating initial construct thickness, which influences oxygen and nutrient diffusion, to more directly tailor subsequent MSC hyaline-like differentiation in vitro. Overall, this cell sheet multilayering technique presents a further platform for continued development of optimized in vitro hyaline-like scaffold-free cartilage transplants and for replacing damaged hyaline articular cartilage rapidly and directly, compared to the current chondrocyte sheet technology. For the future study, we plan to transplant the multi-layered cartilage tissue covering the articular cartilage defect in vivo to verify treatment effects for articular cartilage defect.

Declaration of competing interest

Teruo Okano holds equity in CellSeed, Inc. (Japan) and is an inventor/developer designated on the patent for CellSeed's commercialized temperature-responsive cultureware. No other competing financial interests exist and all authors declare that they have no other competing interests.

Acknowledgements

References

[1] Armiento AR, Alini M, Stoddart MJ. Articular fibrocartilage - why does hyaline cartilage fail to repair? Adv Drug Deliv Rev 2019;146:289–305. https://doi.org/10.1016/j.addr.2018.12.015.
[2] Minas T. A primer in cartilage repair. J Bone Jt Surg Br 2012;94:1482–6. https://doi.org/10.1302/0301-620X.94B11.
[3] Hunziker EB, Lippuner K, Keel MJB, Shintani N. An educational review of cartilage repair: precepts & practice - myths & misconceptions - progress & prospects. Osteoarthritis Cartilage 2015;23:334–50. https://doi.org/10.1016/j.joca.2014.12.011.
[4] Gelber AC, Hochberg MC, Mead LA, Wang N-Y, Wigley FM, Klag MJ. Joint injury in young adults and risk for subsequent knee and hip osteoarthritis. Ann Intern Med 2000;133:321. https://doi.org/10.7326/0003-4819-133-5-200009050-00007.
[5] Sophia Fox AJ, Bedi A, Rodeo SA. The basic science of articular cartilage: structure, composition, and function. Sport Health 2009;1:461–8. https://doi.org/10.1177/1941738109350438.
[6] Thorp H, Kim K, Kondo M, Maak T, Grainger DW, Okano T. Trends in articular cartilage tissue engineering: 3D mesenchymal stem cell sheets as candidates for engineered hyaline-like cartilage. Cells 2021;10:643. https://doi.org/10.3390/cells10030643.
[7] Sato M, Yamato M, Mitani G, Takagaki T, Hamahashi K, Nakamura Y, et al. Combined surgery and chondrocyte cell-sheet transplantation improves

clinical and structural outcomes in knee osteoarthritis. Npj Regen Med 2019;4. https://doi.org/10.1038/s41536-019-0069-4.

[8] Langer R, Vacanti JP. Tissue engineering. Science (80-) 1993;260:920—6. https://doi.org/10.1080/00131725009342110.

[9] Campos Y, Almirall A, Fuentes G, Bloem HL, Kaijzel EL, Cruz LJ. Tissue engineering: an alternative to repair cartilage. Tissue Eng B Rev 2019;25:357—73. https://doi.org/10.1089/ten.teb.2018.0330.

[10] Howard D, Buttery LD, Shakesheff KM, Roberts SJ. Tissue engineering: strategies, stem cells and scaffolds. J Anat 2008;213:66—72. https://doi.org/10.1111/j.1469-7580.2008.00878.x.

[11] Caplan AI. Mesenchymal stem cells. J Orthop Res 1991;9:641—50. https://doi.org/10.1002/jor.1100090504.

[12] Caplan AI, Sorrell JM. The MSC curtain that stops the immune system. Immunol Lett 2015. https://doi.org/10.1016/j.imlet.2015.06.005.

[13] Mackay AM, Beck SC, Murphy JM, Barry FP, Chichester CO, Pittenger MF. Chondrogenic differentiation of cultured human mesenchymal stem cells from marrow. Tissue Eng 1998;4:415—28. https://doi.org/10.1089/ten.1998.4.415.

[14] Kondo M, Kameishi S, Grainger DW, Okano T. Novel therapies using cell sheets engineered from allogeneic mesenchymal stem/stromal cells. Emerg Top Life Sci 2020. https://doi.org/10.1042/etls20200151.

[15] Johnstone B, Hering TM, Caplan AI, Goldberg VM, Yoo JU. In vitro chondrogenesis of bone marrow-derived mesenchymal progenitor cells. Exp Cell Res 1998;238:265—72. https://doi.org/10.1006/excr.1997.3858.

[16] Xu J, Wang W, Ludeman M, Cheng K, Hayami T, Lotz JC, et al. Chondrogenic differentiation of human mesenchymal stem cells in three-dimensional alginate gels. Tissue Eng 2008;14:667—80. https://doi.org/10.1089/tea.2007.0272.

[17] Yamashita A, Nishikawa S, Rancourt DE. Identification of five developmental processes during chondrogenic differentiation of embryonic stem cells. PLoS One 2010. https://doi.org/10.1371/journal.pone.0010998.

[18] Somoza RA, Welter JF, Correa D, Caplan AI. Chondrogenic differentiation of mesenchymal stem cells: challenges and unfulfilled expectations. Tissue Eng B Rev 2014;20:596—608. https://doi.org/10.1089/ten.teb.2013.0771.

[19] Deng Y, Lei G, Lin Z, Yang Y, Lin H, Tuan RS. Engineering hyaline cartilage from mesenchymal stem cells with low hypertrophy potential via modulation of culture conditions and Wnt/β-catenin pathway. Biomaterials 2019;192:569—78. https://doi.org/10.1016/j.biomaterials.2018.11.036.

[20] Blain EJ. Involvement of the cytoskeletal elements in articular cartilage homeostasis and pathology. Int J Exp Pathol 2009;90:1—15. https://doi.org/10.1111/j.1365-2613.2008.00625.x.

[21] Park Y-B, Ha C-W, Rhim JH, Lee H-J. Stem cell therapy for articular cartilage repair: review of the entity of cell populations used and the result of the clinical application of each entity. Am J Sports Med 2018;46:2540—52. https://doi.org/10.1177/0363546517729152.

[22] Yang J, Yamato M, Shimizu T, Sekine H, Ohashi K, Kanzaki M, et al. Reconstruction of functional tissues with cell sheet engineering. Biomaterials 2007;28:5033—43. https://doi.org/10.1016/j.biomaterials.2007.07.052.

[23] Owaki T, Shimizu T, Yamato M, Okano T. Cell sheet engineering for regenerative medicine: current challenges and strategies. Biotechnol J 2014;9:904—14. https://doi.org/10.1002/biot.201300432.

[24] Kushida A, Yamato M, Konno C, Kikuchi A, Sakurai Y, Okano T. Decrease in culture temperature releases monolayer endothelial cell sheets together with deposited fibronectin matrix from temperature-responsive culture surfaces. J Biomed Mater Res 1999;45:355—62. https://doi.org/10.1002/(SICI)1097-4636(19990615)45:4<355::AID-JBM10>3.0.CO;2-7.

[25] Yang J, Yamato M, Kohno C, Nishimoto A, Sekine H, Fukai F, et al. Cell sheet engineering: recreating tissues without biodegradable scaffolds. Biomaterials 2005. https://doi.org/10.1016/j.biomaterials.2005.04.061.

[26] Kim K, Bou-Ghannam S, Okano T. Cell sheet tissue engineering for scaffold-free three-dimensional (3D) tissue reconstruction. Methods Cell Biol. 2020;157:143—67. https://doi.org/10.1016/bs.mcb.2019.11.020. Academic Press Inc.

[27] Kondo M, Kameishi S, Kim K, Metzler NF, Maak TG, Hutchinson DT, et al. Safety and efficacy of human juvenile chondrocyte-derived cell sheets for osteochondral defect treatment. Npj Regen Med 2021;6:1—11. https://doi.org/10.1038/s41536-021-00173-9.

[28] Thorp H, Kim K, Kondo M, Grainger DW, Okano T. Fabrication of hyaline-like cartilage constructs using mesenchymal stem cell sheets. Sci Rep 2020;10. https://doi.org/10.1038/s41598-020-77842-0.

[29] Tsuda Y, Shimizu T, Yamato M, Kikuchi A, Sasagawa T, Sekiya S, et al. Cellular control of tissue architectures using a three-dimensional tissue fabrication technique. Biomaterials 2007;28. https://doi.org/10.1016/j.biomaterials.2007.08.002.

[30] Patel NG, Zhang G. Stacked stem cell sheets enhance cell-matrix interactions. Organogenesis 2014;10:170—6. https://doi.org/10.4161/org.28990.

[31] Kim K, Utoh R, Ohashi K, Kikuchi T, Okano T. Fabrication of functional 3D hepatic tissues with polarized hepatocytes by stacking endothelial cell sheets in vitro. J Tissue Eng Regen Med 2017;11:2071—80. https://doi.org/10.1002/term.2102.

[32] Williams C, Xie AW, Yamato M, Okano T, Wong JY. Stacking of aligned cell sheets for layer-by-layer control of complex tissue structure. Biomaterials 2011;32:5625—32. https://doi.org/10.1016/J.BIOMATERIALS.2011.04.050.

[33] Haraguchi Y, Shimizu T, Sasagawa T, Sekine H, Sakaguchi K, Kikuchi T, et al. Fabrication of functional three-dimensional tissues by stacking cell sheets in vitro. Nat Protoc 2012;7:850—8. https://doi.org/10.1038/nprot.2012.027.

[34] Kaneshiro N, Sato M, Ishihara M, Mitani G, Sakai H, Mochida J. Bioengineered chondrocyte sheets may be potentially useful for the treatment of partial thickness defects of articular cartilage. Biochem Biophys Res Commun 2006;349:723—31. https://doi.org/10.1016/j.bbrc.2006.08.096.

[35] Hamahashi K, Sato M, Yamato M, Kokubo M, Mitani G, Ito S, et al. Studies of the humoral factors produced by layered chondrocyte sheets. J Tissue Eng Regen Med 2015;9:24—30. https://doi.org/10.1002/term.1610.

[36] Kokubo M, Sato M, Yamato M, Mitani G, Kutsuna T, Ebihara G, et al. Characterization of chondrocyte sheets prepared using a co-culture method with temperature-responsive culture inserts. J Tissue Eng Regen Med 2016;10:486—95. https://doi.org/10.1002/term.1764.

[37] Sekine W, Haraguchi Y, Shimizu T, Yamato M, Umezawa A, Okano T. Chondrocyte differentiation of human endometrial gland-derived MSCs in layered cell sheets. Sci World J 2013;2013. https://doi.org/10.1155/2013/359109.

[38] Hasegawa A, Haraguchi Y, Shimizu T, Okano T. Rapid fabrication system for three-dimensional tissues using cell sheet engineering and centrifugation. J Biomed Mater Res 2015;103:3825—33. https://doi.org/10.1002/jbm.a.35526.

[39] Kobayashi J, Kikuchi A, Aoyagi T, Okano T. Cell sheet tissue engineering: cell sheet preparation, harvesting/manipulation, and transplantation. J Biomed Mater Res 2019;107:955—67. https://doi.org/10.1002/jbm.a.36627.

[40] Kikuchi T, Shimizu T, Wada M, Yamato M, Okano T. Automatic fabrication of 3-dimensional tissues using cell sheet manipulator technique. Biomaterials 2014. https://doi.org/10.1016/j.biomaterials.2013.12.014.

[41] Li JJ, Kim K, Roohani-Esfahani SI, Guo J, Kaplan DL, Zreiqat H. A biphasic scaffold based on silk and bioactive ceramic with stratified properties for osteochondral tissue regeneration. J Mater Chem B 2015;3:5361—76. https://doi.org/10.1039/c5tb00353a.

[42] Schmitz N, Laverty S, Kraus VB, Aigner T. Basic methods in histopathology of joint tissues. Osteoarthritis Cartilage 2010;18:S113—6. https://doi.org/10.1016/j.joca.2010.05.026.

[43] Schmittgen TD, Livak KJ. Analyzing real-time PCR data by the comparative C(T) method. Nat Protoc 2008;3:1101—8. https://doi.org/10.1038/nprot.2008.73.

[44] Watts AE, Ackerman-Yost JC, Nixon AJ. A comparison of three-dimensional culture systems to evaluate in vitro chondrogenesis of equine bone marrow-derived mesenchymal stem cells. Tissue Eng 2013;19:2275—83. https://doi.org/10.1089/ten.tea.2012.0479.

[45] Merceron C, Portron S, Masson M, Lesoeur J, Fellah BH, Gauthier O, et al. The effect of two- and three-dimensional cell culture on the chondrogenic potential of human adipose-derived mesenchymal stem cells after subcutaneous transplantation with an injectable hydrogel. Cell Transplant 2011;20:1575—88. https://doi.org/10.3727/096368910X557191.

[46] Von Der Mark K, Gauss V, Von Der Mark H, Müller P. Relationship between cell shape and type of collagen synthesised as chondrocytes lose their cartilage phenotype in culture. Nature 1977;267:531—2. https://doi.org/10.1038/267531a0.

[47] Hall AC. The role of chondrocyte morphology and volume in controlling phenotype—implications for osteoarthritis, cartilage repair, and cartilage engineering. Curr Rheumatol Rep 2019;21:38. https://doi.org/10.1007/s11926-019-0837-6.

[48] Bou-Ghannam S, Kim K, Grainger DW, Okano T. 3D cell sheet structure augments mesenchymal stem cell cytokine production. Sci Rep 2021;11:8170. https://doi.org/10.1038/s41598-021-87571-7.

[49] DeLise AM, Fischer L, Tuan RS. Cellular interactions and signaling in cartilage development. Osteoarthritis Cartilage 2000;8:309—34. https://doi.org/10.1053/joca.1999.0306.

[50] Millward-Sadler SJ, Salter DM. Integrin-dependent signal cascades in chondrocyte mechanotransduction. Ann Biomed Eng 2004;32:435—46. https://doi.org/10.1023/B:ABME.0000017538.72511.48.

[51] Coelho CND, Kosher RA. Gap junctional communication during limb cartilage differentiation. Dev Biol 1991;144:47—53. https://doi.org/10.1016/0012-1606(91)90477-K.

[52] Tavella S, Raffo P, Tacchetti C, Cancedda R, Castagnola P. N-CAM and N-cadherin expression during in vitro chondrogenesis. Exp Cell Res 1994;215:354—62. https://doi.org/10.1006/excr.1994.1352.

[53] Rossello RA, Kohn DH. Cell communication and tissue engineering. Commun Integr Biol 2010;3:64—6. https://doi.org/10.4161/cib.3.1.10141.

[54] Green JD, Tollemar V, Dougherty M, Yan Z, Yin L, Ye J, et al. Multifaceted signaling regulators of chondrogenesis: implications in cartilage regeneration and tissue engineering. Genes Dis 2015;2:307—27. https://doi.org/10.1016/j.gendis.2015.09.003.

[55] Kino-oka M, Ngo TX, Nagamori E, Takezawa Y, Miyake Y, Sawa Y, et al. Evaluation of vertical cell fluidity in a multilayered sheet of skeletal myoblasts. J Biosci Bioeng 2012;113:128—31. https://doi.org/10.1016/j.jbiosc.2011.09.001.

[56] Ling L, Nurcombe V, Cool SM. Wnt signaling controls the fate of mesenchymal stem cells. Gene 2009;433:1—7. https://doi.org/10.1016/j.gene.2008.12.008.

[57] Barker N, Van Den Born M. Detection of β-catenin localization by immunohistochemistry. Methods Mol Biol 2008;468:91—8. https://doi.org/10.1007/978-1-59745-249-6_7.

[58] Farrell MJ, Comeau ES, Mauck RL. Mesenchymal stem cells produce functional cartilage matrix in three- dimensional culture in regions of optimal nutrient supply. Eur Cell Mater 2012;23:425—40. https://doi.org/10.22203/eCM.v023a33.

[59] Rouwkema J, Koopman BFJM, Van Blitterswijk CA, Dhert WJ, Malda J. Supply of nutrients to cells in engineered tissues. Biotechnol Genet Eng Rev 2009;26: 163—78. https://doi.org/10.5661/bger-26-163.

[60] Haraguchi Y, Sekine W, Shimizu T, Yamato M, Miyoshi S, Umezawa A, et al. Development of a new assay system for evaluating the permeability of various substances through three-dimensional tissue. Tissue Eng C Methods 2010;16: 685—92. https://doi.org/10.1089/ten.tec.2009.0459.

[61] Sekine W, Haraguchi Y. Thickness limitation and cell viability of multi-layered cell sheets and overcoming the diffusion limit by a porous-membrane culture insert. J Biochips Tissue Chips 2011;1. https://doi.org/10.4172/2153-0777.s1-007.

[62] McMurtrey RJ. Analytic models of oxygen and nutrient diffusion, metabolism dynamics, and architecture optimization in three-dimensional tissue constructs with applications and insights in cerebral organoids. Tissue Eng C Methods 2016;22:221—49. https://doi.org/10.1089/ten.tec.2015.0375.